Real-Time Subcarrier Cluster-Based Adaptive Modulation for Underwater Acoustic OFDM Communication

Suchi Barua, Yue Rong, Sven Nordholm, Peng Chen
School of Electrical Engineering, Computing and Mathematical Sciences
Curtin University, Bentley, WA 6102, Australia

***Abstract*— Adaptive modulation is appealing for underwater acoustic (UA) communication system in order to improve the system efficiency. High data rate communication is challenging as underwater channels are fast varying according to environmental conditions. Self-adapting systems can select the best technique for time-varying underwater channel based on the channel condition to guarantee continuous connectivity and optimal performance all the time. This paper presents a real-time orthogonal frequency-division multiplexing (OFDM) based adaptive UA communication system, implemented using the National Instruments (NI) CompactDAQ device and the LabVIEW software. The signal-to-noise ratio (SNR) is calculated at the receiver for clusters (group of subcarriers) to reduce the computational and feedback load and used as a performance metric to switch the modulation mode of each cluster which is fed back to the transmitter for data transmission. The experimental results verify the superiority of the proposed adaptive scheme.**

Keywords—Adaptive modulation, time-varying channel, underwater acoustic communication, LabVIEW, CompactDAQ, orthogonal frequency-division multiplexing (OFDM).

Global Oceans 2020: Singapore - U.S. Gulf Coast | 978-1-7281-5446-6/20/$31.00 ©2020 IEEE | DOI: 10.1109/IEEECONF38699.2020.9389157

I. INTRODUCTION

The underwater acoustic (UA) channel is considered as one of the most difficult channels for reliable communication because of randomly varying multi-path propagation, rapid time-variation, severe fading due to limited bandwidth, refractive properties of the medium and large Doppler shifts due to motion [1]. Orthogonal frequency-division multiplexing (OFDM) is an efficient technique for UA communications because of its remarkable capability in mitigating multipath interference with a low computational complexity [1-3]. We develop a communication system employing adaptive modulation scheme for nonstationary environment such as UA channel to improve the reliability of communication and boost data rate.

In non-adaptive (fixed) modulation, the transmitter does not exploit any information on the available channel parameters in choosing the modulation scheme. Alternatively, the channel information is made available to the transmitter in adaptive modulation and the performance of an adaptive modulation scheme depends on the transmitter's knowledge of the channel which is fed back from the receiver to the transmitter [4-6].

In this paper, OFDM and adaptive modulation and coding technique is considered in order to achieve high spectral efficiency. Cluster-based adaptive modulation is chosen to reduce the computational complexity and feedback load of the adaptive scheme [5]. Signal-to-noise ratio (SNR) is estimated at the receiver for each group of subcarriers (i.e. cluster). The received cluster SNR is used as the channel state information (CSI) to choose the adaptive allocation of the transmission parameters for each cluster, which are sent back to the transmitter for the next data frame. If the received cluster SNR falls below the threshold, the data subcarriers in those clusters are considered as weak subcarriers and discarded for the next transmission and the remaining data subcarriers are transmitted with different modulation constellations depending on the received cluster SNR for the next data frame and thus higher data rate and better power and spectral efficiency can be achieved.

Adaptive modulation becomes challenging with the increase of the Doppler frequency which leads to significant inter-carrier interference (ICI). ICI deteriorates the system performance resulting in low received SNR as it increases the power of received signal in the inactive (null) subcarriers and also misleads the detection of transmitted signal on active subcarriers [7]. Thus the ICI affects the estimation of SNR, which in turn affects the performance of adaptive modulation. During the experiment the estimation of carrier frequency offset (CFO) is bypassed as the Doppler shift is very low in tank.

In this paper, a combination of the National Instruments (NI) LabVIEW software and CompactDAQ device is adopted for real-time adaptive modulation for UA OFDM communication and its performance using the real-time tank experiment is studied. The system design including both the transmitter and receiver is discussed.

The rest of the paper is organised as follows. The system model is introduced in Section II. The channel model is presented in Section III. The adaptive modulation implementation is presented in Section IV. The real-time system implementation is described in Section V. The experimental results are discussed in Section VI. Conclusion is presented in Section VII.

II. SYSTEM MODEL

A frame-based UA OFDM communication system is considered in this paper. The frame structure of the transmitted signals is shown in Fig. 1.

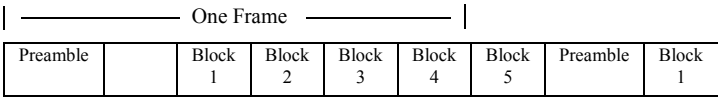

Fig. 1. Frame structure of the UA OFDM system.

Each frame contains five OFDM data blocks and one preamble block. Each data block contains pilot subcarriers,

978-1-7281-5446-6/20/$31.00 ©2020 IEEE
Authorized licensed use limited to: CURTIN UNIVERSITY. Downloaded on April 30,2021 at 02:48:42 UTC from IEEE Xplore. Restrictions apply.

null subcarriers and data subcarriers. The preamble block is used for synchronization [2, 3, 8]. In each frame, a binary source data stream $\boldsymbol{d} = (d[1], \dots, d[K_d])^T$ is generated, where $(\cdot)^T$ denotes the matrix (vector) transpose, K_d is the number of information-carrying bits in each frame. Each OFDM symbol is converted to the time domain by the inverse discrete Fourier transform (DFT), leading to the following baseband discrete time signal

$$\boldsymbol{x} = \boldsymbol{F}^H \boldsymbol{s} \tag{1}$$

where $(\cdot)^H$ denotes the conjugate transpose and $\boldsymbol{F}$ is a $K_s \times K_s$ DFT matrix, $\boldsymbol{s} = (s[1], \dots, s[K_s])^T$ is the OFDM symbol vector mapped from $\boldsymbol{d}$ depending on modulation constellations and K_s is the number of total subcarriers. The bandwidth of the transmitted signal is $B = f_{sc}K_s$, where f_{sc} is the subcarrier spacing. The duration of one OFDM symbol is $T = 1/f_{sc}$ and the total length of one OFDM block is $T_{total} = T + T_{cp}$, where T_{cp} is the length of cyclic prefix (CP). After removing the CP at the receiver end, the baseband discrete time samples of one OFDM symbol is

$$\boldsymbol{r}_t = \boldsymbol{P}\boldsymbol{F}^H\boldsymbol{S}\boldsymbol{F}\boldsymbol{h}_t + \boldsymbol{w}_t \tag{2}$$

where $\boldsymbol{S} = diag\,(\boldsymbol{s})$ is a diagonal matrix and $\boldsymbol{w}_t = (w[1], \dots w[K_s])^T$ is the additive noise vector, $\boldsymbol{h}_t$ is the discrete time domain representation of the channel impulse response (CIR) and $\boldsymbol{P} = diag\,(1, e^{-j2\pi\epsilon/B}, \dots, e^{-j2\pi(K_s-1)\epsilon/B})^T$ is the phase distortion caused by the Doppler shift and ϵ is CFO.

After estimating and removing the frequency offset, the frequency domain representation of the received signal is

$$\boldsymbol{r}_f = \boldsymbol{S}\boldsymbol{h}_f + \boldsymbol{w}_f \tag{3}$$

where $\boldsymbol{w}_f$ is the additive noise vector in the frequency domain. $\boldsymbol{h}_f = (h_f[1], \dots . h_f[K_s])^T$ is a vector containing the channel frequency response (CFR) at all K_s subcarriers [9].

III. Channel Model

UA communication is challenging because of the unique characteristics of UA channel and considered as one of the most difficult communication channels due to the rapid dispersion in both time and frequency domain. UA channels are generally characterized by randomly time-varying multipath propagation which results in frequency selective fading. Additionally, motion of the transmitter and/or receiver introduces the Doppler shift to the channel which contributes to the changes in CIR. The CIR can be defined as

$$h(\tau, t) = \sum_{p=1}^{N_p} h_p(t)\delta(\tau - \tau_p(t)) \tag{4}$$

where N_p is the number of propagation path, τ is delay, $\delta(.)$ is the Dirac delta function and t is the time at which the channel is observed. The coefficient $h_p(t)$ represents the gain of the pth path and $\tau_p(t)$ is the corresponding time-varying delay [10, 11].

The CFR is expressed as

$$h_f(t) = \sum_{p=1}^{N_p} h_p(t)\, e^{-j2\pi f \tau_p(t)} \tag{5}$$

A. CFO Estimation

In this paper, it is assumed that the motion of the transmitter and/or the receiver is causing the dominant Doppler shift. After removing CP from the received signal, CFO is estimated in null subcarriers in the receiver side. The CFO is performed in each OFDM block. The energy of the null subcarriers is used as the cost function.

$$J(\epsilon) = |\boldsymbol{\Theta}\boldsymbol{F}\boldsymbol{\Gamma}^H(\epsilon)\boldsymbol{r}_t|^2 \tag{6}$$

where $\boldsymbol{\Theta}$ is a selection matrix that picks the frequency-domain measurements on the null subcarriers out of all K_s subcarriers, $||$ is the Euclidean norm of a vector, $\boldsymbol{\Gamma}(\epsilon) = diag\,(1,\ e^{j2\pi T_c\epsilon}, \dots, e^{j2\pi T_c(K_s-1)\epsilon})$ is diagonal matrix where $T_c = 1/B$ is the time interval for each sample. An estimation of ϵ is found through

$$\hat{\epsilon} = argmin\, J(\epsilon) \tag{7}$$

which is solved via 1-D search for ϵ [7].

Doppler shift is a limiting factor in UA communication which leads to ICI because signal components from one subcarrier spill over to the immediate neighbouring subcarriers. With the increase of Doppler frequency, the ICI increases the power of the received signal on inactive subcarriers. As a result the possibility of erroneous detection of subcarriers state enhances and in turn misleads the detection of transmitted symbols on the active subcarriers. ICI-free reception can be approximately achieved with this high-resolution algorithm which is similar to the MUSIC-like algorithm proposed in [12] for CP-OFDM.

IV. Adaptive Modulation

In this paper, the subcarriers of the OFDM blocks are grouped into clusters. Each cluster consists of active subcarriers (data and pilot subcarriers). The active subcarriers $\mathcal{K}_a$ where $\mathcal{K}_a = \mathcal{K}_p \cup \mathcal{K}_d$ [1] is grouped into Q clusters. The size of each cluster in each OFDM block is K_a/Q. To keep the same size of each cluster the active subcarriers are grouped in 22 clusters in this experiment where the size of each cluster is 20 including 5 pilot subcarriers and 15 data subcarriers.

Following the OFDM signal design, noise and received signal power is measured in the frequency domain at the receiver. Received power at null subcarriers is used for noise variance estimation as

$$\hat{\sigma}_n^2 = \frac{1}{\bar{\mathcal{K}}_n} \sum_{m=1}^{\bar{\mathcal{K}}_n} \left| r_f[\mathcal{K}_n(m)] \right|^2 \tag{8}$$

where $\mathcal{K}_n$ is the set containing the indices of null subcarriers and for a set $\mathcal{X}$, $\bar{\mathcal{X}}$ denotes the number of elements in $\mathcal{X}$ and $r_f[m]$ is the frequency-domain received signal at the m th subcarrier. The SNR of each cluster in the frequency domain can be estimated as

Authorized licensed use limited to: CURTIN UNIVERSITY. Downloaded on April 30,2021 at 02:48:42 UTC from IEEE Xplore. Restrictions apply.

$$\bar{\gamma}_q = \frac{\frac{1}{\bar{\mathcal{K}}_{a_q}} \sum_{m_q=1}^{\bar{\mathcal{K}}_{a_q}} \left| r_f[\mathcal{K}_{a_q}(m_q)] \right|^2}{\frac{1}{\bar{\mathcal{K}}_n} \sum_{m=1}^{\bar{\mathcal{K}}_n} \left| r_f[\mathcal{K}_n(m)] \right|^2} - 1 \quad (9)$$

where $\mathcal{K}_{a_q}$ is the set containing the indices of pilot and data subcarriers of each cluster. If the received SNR of a cluster is less than the target SNR, then the data subcarriers of this cluster are discarded from the next transmitted frame. If the received SNR of a cluster is greater than the target SNR, we keep the data subcarriers of this cluster and send the transmitter adaptively allocated parameters (modulation mode) for the next transmission. This method is shown in Fig. 2.

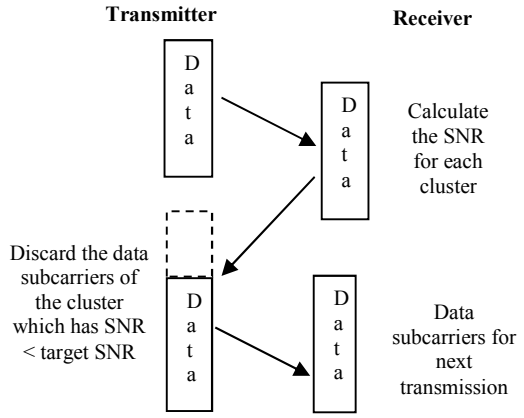

Fig. 2. Discarding data subcarriers depending on the SNR estimation.

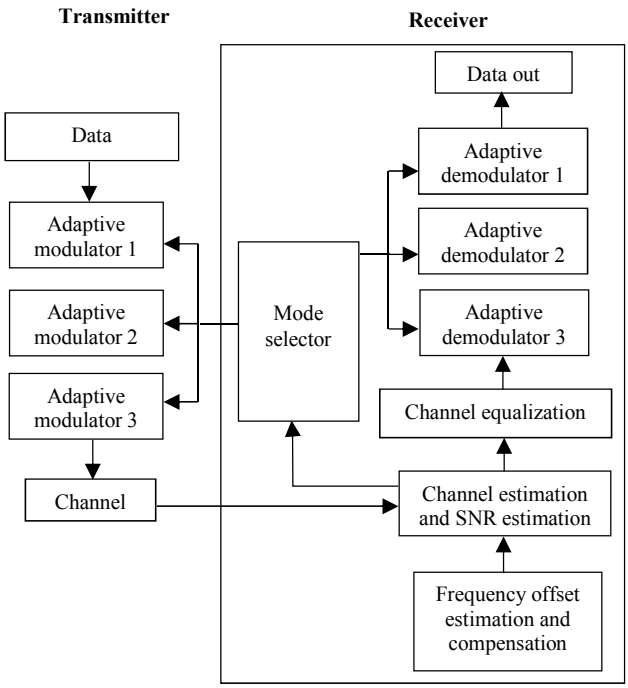

Fig. 3. Block diagram of adaptive modulation scheme.

The block diagram of the proposed adaptive modulation scheme in Fig. 3 shows that frequency offset estimation and compensation are done at the receiver side. Then channel estimation and SNR estimation are performed. Then modulation modes are selected for the remaining clusters by the mode selector block depending on the estimated cluster SNR and fed back to the transmitter. The adaptive modulator/demodulator blocks consist of different modulators/demodulators which modulate/demodulate the equalized data subcarriers of the clusters according to the selected mode.

In this work, the adaptation is done frame by frame. Individual modulation scheme results have been observed and analyzed for UA communication systems with fixed modulation. Experiment results of fixed modulation for different modulation schemes are used to select the target bit-error-rate (BER) and the estimated average cluster SNR is used as switching parameter [4, 13]. Here, we would like to note that the estimated received SNR reflects the effect of Doppler frequency. The SNR estimation algorithm performs better at lower Doppler frequency than the higher Doppler frequency which is shown in [14]. Switching threshold for the adaptive modulation system is determined to keep the overall BER lower than the target BER. In fact, the highest modulation order is chosen under a certain BER and SNR. Therefore, a better tradeoff between data rate and overall BER is achieved by the proposed adaptation system.

V. System Implementation

A. System Hardware

An NI CompactDAQ data generation and acquisition system is adopted in our experiment which is capable of analog I/O, digital I/O, counter/timer operations, and industrial bus communication. It consists of a chassis and NI I/O modules. In the CompactDAQ system, an NI cDAQ-9174 plug-and-play chassis is connected to a laptop through USB where the NI LabVIEW software is installed for the signal generation, acquisition and processing. It is a four slot chassis which controls the timing, synchronization, and data transfer among up to four I/O modules and the external host (computer).

An NI-9260, 2-channel voltage output module and an NI-9232, 3-channel dynamic signal acquisition module are plugged into two of the four slots of the chassis for signal generation and acquisition respectively. The CTG0052 acoustic transducer is connected to the NI-9260 module through a transformer matching network and a power amplifier to transmit acoustic signals through the UA channel. The Reson reference and HTI-96-Min hydrophones are connected to the NI-9232 modules through preamplifiers to acquire signals received from the UA channel for the forward and feedback links respectively. For adaptive modulation two sets of devices are used. One set is designed for the forward link and the other set is designed for the feedback link.

B. Software Implementation

The software of our adaptive UA OFDM system is designed and implemented using NI LabVIEW. The system parameters used in the experiment are listed in Table I. The system generates one frame and forwards the generated data frame to channel 1 of NI 9260 (DAQ1/Slot2/channel1). The CTG0052 (1) transducer transmits the signal through the UA channel. Then the Reson reference hydrophone receives the signal and forwards the received data to NI9232

Authorized licensed use limited to: CURTIN UNIVERSITY. Downloaded on April 30,2021 at 02:48:42 UTC from IEEE Xplore. Restrictions apply.

(DAQ2/Slot1/channel1). Then the signal is processed by the receiver in LabVIEW.

received data to NI9232 (DAQ1/Slot1/channel1) for processing. The real-time adaptive modulation scheme is shown in Fig. 4.

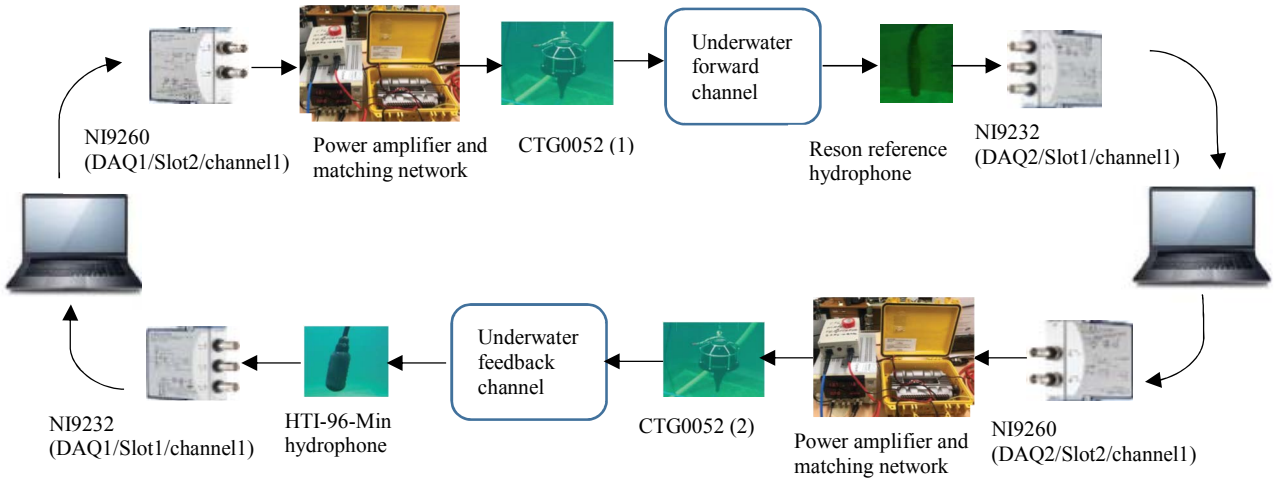

Fig. 4. LabVIEW-based implementation of real-time adaptive modulation for UA OFDM system.

TABLE I. PARAMETERS USED IN EXPERIMENT

Bandwidth	B = 4 kHz
Number of subcarriers	K_s = 512
Subcarrier spacing	f_{sc} = 7.8 Hz
Length of OFDM symbol	T = 128 ms
Length of CP	T_{cp} = 25 ms
Number of pilot subcarriers	K_p = 110
Number of data subcarriers	K_d = 330
Number of null subcarriers	K_n = 72

At first, the signal samples received by NI9232 are converted from the passband to the baseband. The receiver then removes the CP from each OFDM block. Then the frequency offset estimation and compensation is performed for each OFDM symbol using the null subcarriers. After that the baseband signals are passed through channel estimation and SNR estimation. The least-squares (LS) method is used to estimate the frequency domain channel response at the pilot subcarriers. The estimated channel response is used to equalize the received signals. Demodulation operation is performed to the equalized signals.

After estimating the cluster SNR of the received signal, the weak clusters are discarded and modulation sizes are selected for remaining clusters depending on the channel condition for the next frame transmission. Data symbols containing the modulation size information are modulated by QPSK constellations and forwarded to NI-9260 (DAQ2/Slot2/channel 1). The CTG0052 (2) transducer feeds back the modulation size information signal through the UA feedback channel. The HTI-96-Min hydrophone receives the modulation size signal and forwards the

VI. EXPERIMENT RESULTS AND DISCUSSION

In the tank experiment, one-way (fixed modulation) experiment is performed for BPSK, QPSK and 16QAM modulations to select the target SNR. This one-way experiment is performed using one pair of transducer and hydrophone. The received SNR is varied through varying the power of the transmitted signal. The target SNR is chosen by plotting the average received cluster SNR vs BER results which is shown in Fig. 5. For the tank experiment, the target uncoded bit-error-rate (BER) is determined as 0.02 for the adaptive modulation scheme. Switching thresholds for the adaptive modulation scheme are presented in Table II.

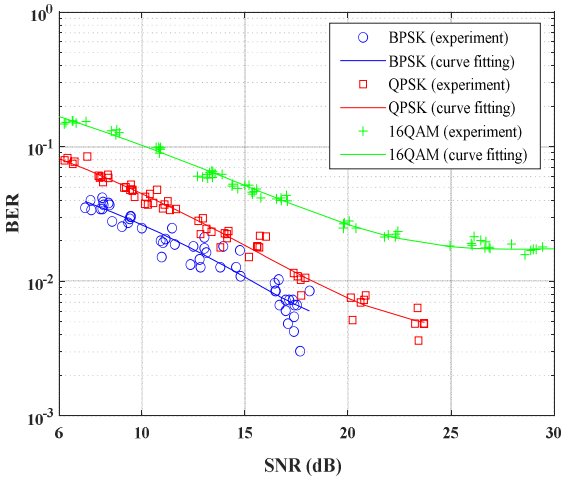

Fig. 5. BER performance of the fixed modulation schemes in tank experiment.

After determining the target SNR, the experiment of adaptive modulation is performed by placing another pair of transducer and hydrophone in the tank. Fig. 6 shows the location of the transducers and hydrophones in the tank during the adaptive modulation experiment. The length, width and depth of the tank are 2.5 m, 1.5m and 1.8 m

Authorized licensed use limited to: CURTIN UNIVERSITY. Downloaded on April 30,2021 at 02:48:42 UTC from IEEE Xplore. Restrictions apply.

respectively. The water depth is 1.2 m. The distance between the forward link and feedback link is 1.85 m. During the experiment, we bypassed the frequency offset estimation and compensation module in Fig. 3 as the Doppler shift is very small in a tank.

TABLE II. SWITCHING THRESHOLDS FOR ADAPTIVE MODULATION SCHEMES

Mode	Decision	Threshold
1	Discard	SNR $<$ 13 dB (target SNR)
2	BPSK	13 $\leq$ SNR $<$ 16 dB
3	QPSK	16 $\leq$ SNR $<$ 25 dB
4	16QAM	SNR $\geq$ 25 dB

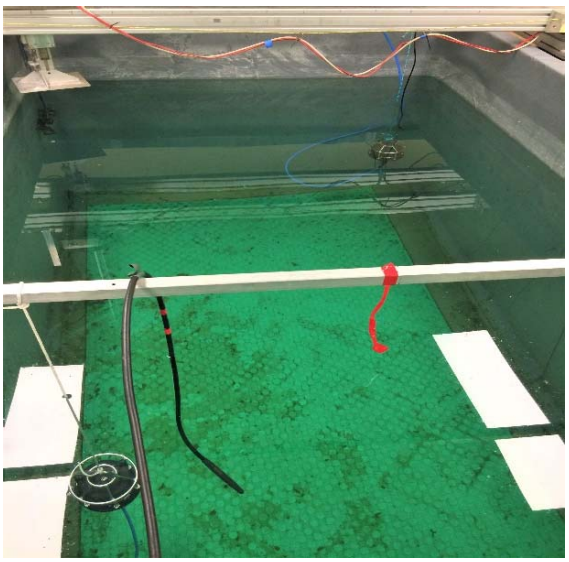

Fig. 6. Location of the transducers and hydrophones for forward and feedback links.

Figs. 7 (a) and (b) show the CFR and respective loaded bits in the clusters of the 3rd OFDM block of a received frame. It can be seen that the number of loaded bits i.e. modulation size for clusters are closely related to the CFR results. When the amplitude of the subcarrier cluster is higher the selected modulation size is also higher and vice versa. Fig. 8 shows how the number of uncoded bits for each transmitted frame varies with channel condition for average received SNR of 13.2 dB, 22.1 dB and 26 dB. It can be seen that, when the average received SNR is close to the target SNR i.e. 13 dB, the number of uncoded bits is reduced as data subcarriers which are under the target SNR are discarded. By discarding the data subcarriers, the system saves the energy which is required to transmit the weak data subcarriers. Fig. 9 shows adaptively loaded bits (0 for discarded, 1 for BPSK, 2 for QPSK and 4 for 16QAM) with the received cluster SNR. The number of loaded bits increases with the increase of the SNR. From Fig. 10, it can be seen that the data rate also increases with increase of the average received SNR.

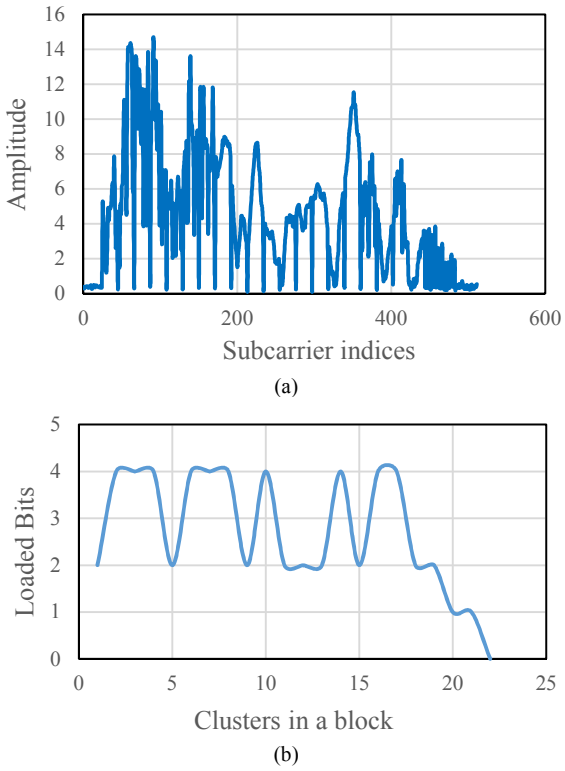

Fig. 7. (a) Channel frequency response and (b) Loaded bits of the 3rd OFDM block of a received frame.

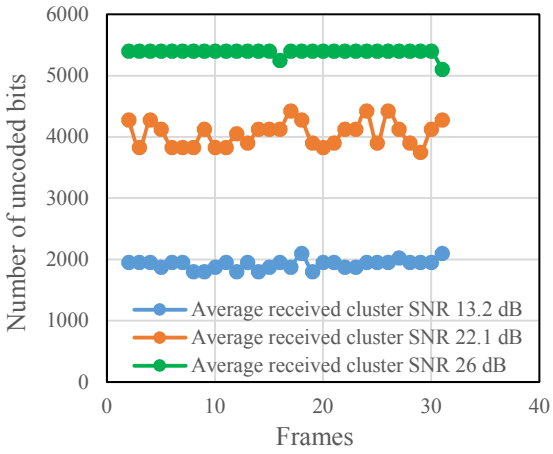

Fig. 8. Number of uncoded bits for each transmitted frame.

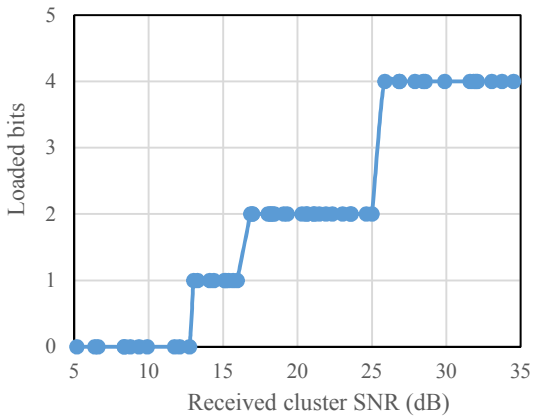

Fig. 9. Loaded bits with the received cluster SNR.

Authorized licensed use limited to: CURTIN UNIVERSITY. Downloaded on April 30,2021 at 02:48:42 UTC from IEEE Xplore. Restrictions apply.

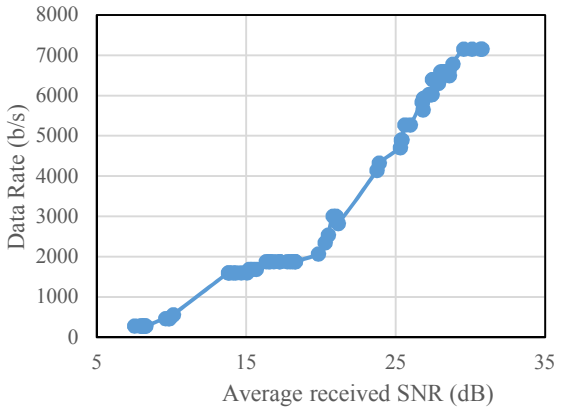

Fig. 10. Data rate of the proposed adaptive modulation system.

VII. Conclusion

In this paper, received SNR is chosen as the CSI to choose the adaptive allocation of the transmission parameters for next transmission. Channel variation as well as Doppler effects are reflected in the received SNR. Cluster-based adaptive modulation scheme is considered to reduce the computational and feedback load. It can be said that the proposed adaptive system is an energy efficient system which reduces the bit energy consumption, guarantees continuous connectivity and ensures higher data rate for a nonstationary time-varying UA channel.

Acknowledgment

This research is supported by an Australian Government Research Training Program (RTP) Stipend and RTP Fee-Offset Scholarship through Curtin University. We also want to thank CMST, Curtin for providing support for tank experiment.

References

[1] S. Zhou and Z. Wang, "OFDM for underwater acoustic communications", John Wiley & Sons Ltd, 2014.

[2] P. Chen, Y. Rong, S. Nordholm, Z. He, and A. Duncan, "Joint channel estimation and impulsive noise mitigation in underwater acoustic OFDM communication systems," IEEE Trans. Wireless Commun., vol. 16, pp. 6165-6178, Sep. 2017.

[3] P. Chen, Y. Rong, S. Nordholm, and Z. He, "Joint channel and impulsive noise estimation in underwater acoustic OFDM systems," IEEE Trans. Veh. Technol., vol. 66, pp. 10567-10571, Nov. 2017.

[4] L. Wan, H. Zhou, X. Xu, Y. Huang, S. Zhou, Z. Shi, and J.H. Cui, "Adaptive modulation and coding for underwater acoustic OFDM", IEEE J. of Oceanic Engineering, vol. 40, issue 2, pp. 327-336, Apr. 2015.

[5] A. Radosevic, R. Ahmed, T. M. Duman, J. G. Proakis, and M. Stojanovic, "Adaptive OFDM modulation for underwater acoustic communication: Design considerations and experimental results", IEEE J. of Oceanic Engineering, vol. 39, no. 2, pp. 357-370, Apr. 2014.

[6] M. Sadeghi, M. Elamassie, and M. Uysal, "Adaptive OFDM-based acoustic underwater transmission: System design and experimental verification," Proc. IEEE International Black Sea Conference on Communications and Networking, Istanbul, pp. 1-5, 2017.

[7] M. Huang, S. Sun, E. Cheng, X. Kuai, and X. Xu, "Joint interference mitigation with channel estimated in underwater acoustic OFDM system", TELKOMNIKA, vol. 11, no. 12, pp. 7423-7430, 2013.

[8] P. Chen, Y. Rong, S. Nordholm, and Z. He, "An Underwater Acoustic OFDM System Based on NI CompactDAQ and LabVIEW", IEEE Systems Journal, vol. 13, pp. 3858-3868, Dec. 2019.

[9] P. Chen, Y. Rong, and S. Nordholm, "Pilot-subcarrier based impulsive noise mitigation for underwater acoustic OFDM systems," in Proc. WUWNet, 2016, Shanghai, China, Oct. 2016.

[10] M. Stojanovic and J. Preisig, "Underwater acoustic communication channels: Propagation models and statistical characterization", IEEE Communications Magazine, vol. 47, no. 1, pp. 84-89, Jan. 2009.

[11] A. Radosevic, T. M. Duman, J. G. Proakis, and M. Stojanovic, "Channel prediction for adaptive modulation in underwater acoustic communications," OCEANS 2011 IEEE, Spain, Santander, pp. 1-5, 2011.

[12] U. Tureli and H. Liu, "A high-efficiency carrier estimator for OFDM communications," IEEE Commun. Lett. vol. 2, no. 4, pp. 104–106, Apr. 1998.

[13] K. Pelekanakis, L. Cazzanti, G. Zappa, and J. Alves, "Decision tree-based adaptive modulation for underwater acoustic communications", 2016 IEEE Third Underwater Communications and Networking Conference (UComms), Lerici, pp. 1-5, 30 Aug.-1 Sept. 2016.

[14] S. Barua, Y. Rong, S. Nordholm, and P. Chen, "Adaptive modulation for underwater acoustic OFDM communication", Proc. MTS/IEEE OCEANS, Marseille, France, June 17-20, 2019.

Authorized licensed use limited to: CURTIN UNIVERSITY. Downloaded on April 30,2021 at 02:48:42 UTC from IEEE Xplore. Restrictions apply.